

Increase the reliability of the device when duplicating the functions of individual nodes★

Andriy Sverstiuk^{1,2,*†}, Taras Dubynyak^{2†}, Petro Mykulyk^{2†}, Volodymyr Nevozhai^{2†} and Oles Hospodarsky^{3†}

¹ I. Horbachevsky Ternopil National Medical University, Maidan Voli, 1, Ternopil, 46002, Ukraine

² Ternopil National Ivan Puluj Technical University, Rus'ka str. 56, Ternopil, 46001, Ukraine

³ National University "Lviv Polytechnic", S.Bandera str, 12, Lviv, 79013, Ukraine

Abstract

This study covers the calculation of a multi-channel adaptive information and measurement system for measuring steam flow to a turbine using the ITABAR probe. The reliability, stability and efficiency of the information system are evaluated, and its accuracy characteristics are determined. The work provides a basis for the design of such an information and measurement system based on the developed schematic diagrams and calculations of the characteristics of the analog-to-digital converter and power that will meet the defined accuracy and reliability. The study also covers the implementation of this system for displaying parameters for the purpose of process control. All necessary engineering calculations will support the proposed design.

Keywords

ITABAR probe, multichannel adaptive information and measurement system IMS

1. Introduction

One of the main characteristics of modern information and measurement systems (IMS) is their reliability. It is reliability that determines the ability of the system to operate continuously and without errors in critical environments, such as nuclear power plants or other facilities with increased safety requirements. To achieve this, various technical solutions are used, one of which is to duplicate the functions of individual units and components. The duplication method allows to guarantee the system's operability even when one or more components fail. Thanks to this approach, the system can continue to perform its functions without interrupting the process or significantly deteriorating technical indicators, which further helps to prevent emergencies.

In modern information systems, the task of duplicating sensors that monitor critical parameters, such as steam flow to the turbine, which is an integral part of the power process at a nuclear power plant, becomes especially important. The sensors based on ITABAR probe technology used in this study provide high measurement accuracy due to their well-thought-out design and minimal pressure losses in the pipeline. However, it is possible to increase the reliability of the system by duplicating them: this allows for a backup for measurements in the event of a malfunction of one of the sensors, which makes the system more resistant to failure and more efficient in long-term operation. The methodology for ensuring reliability through redundancy has been carefully

ICyberPhyS'25: 2nd International Workshop on Intelligent & CyberPhysical Systems, July 04, 2025, Khmelnytskyi, Ukraine

★ Corresponding author.

† These authors contributed equally.

✉ sverstyuk@tdmu.edu.ua (A. Sverstiuk); d_taras@ukr.net (T. Dubyniak); mykpet7@gmail.com (P. Mykulyk); v.nevo1971@gmail.com (V. Nevozhai); hospodarskyoles@gmail.com (O. Hospodarsky)

ORCID 0000-0001-8644-0776 (A. Sverstiuk); 0000-0003-1529-6951 (T. Dubyniak); 0000-0001-6008-6510 (Petro Mykulyk); 0009-0004-2003-4280 (V. Nevozhai); 0009-0005-9088-3015 (O. Hospodarsky)



© 2025 Copyright for this paper by its authors. Use permitted under Creative Commons License Attribution 4.0 International (CC BY 4.0).

considered, using differential equations to model possible transitions between system states, which makes it possible to accurately predict the system's operation under certain conditions.

The Itabar probe receives and averages dynamic and static pressures at four points distributed across the pipeline cross-section [1-4]. Therefore, the asymmetry of the flow profile has only a minor effect on the measurement result, making it possible to obtain accurate measurement results even with short free areas. The following free areas are typical:

- diameters after 90° rotation;
- diameters after two turns in the same plane;
- diameters after narrowing or expanding the pipeline;

Low installation costs. To install an Itabar probe, all that is required is a simple socket through which the probe can be inserted into the pipeline. The spigot is attached with a welded seam with a length of approximately 100 mm, depending on the type of probe. The probe is much smaller and lighter than a diaphragm. This results in significant savings in working time and labor costs. The detachable version of the Itabar probe is particularly advantageous in this regard. The savings in installation tools compared to a diaphragm reach 25% for small pipe diameters and more than 70% for large ones [5].

Lower pressure loss and thus lower energy costs. The hydraulically advantageous shape of the Itabar probe creates virtually no flow line constriction and thus creates the lowest residual pressure loss compared to other primary flow measuring devices. The pressure loss on the Itabar probe is no more than 15% of the measured differential pressure value. This is quite a good value compared to the pressure loss at the diaphragm, which is typically 60% of the measured differential pressure Figure 1.

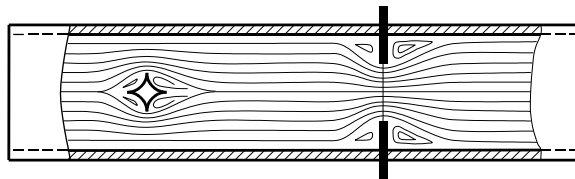


Figure 1: Effect of Itabar probe and diaphragm on flow.

1.1. Itabar probe for flow measurement

The principle of measurement is based on Bernoulli's law, which states that the sum of the energy due to the pressure in the pipe, the potential energy and the kinetic energy at each point in the pipe at any given time remains constant if we consider a stationary flow and neglect friction [6] Figure 2.

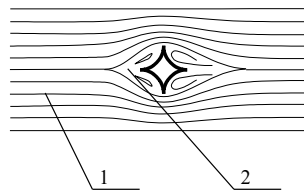


Figure 2: The effect of the Itabar probe on the flow shape (1 - linear flow, 2 - obstacle flow).

$$P + \frac{\sigma}{2} \cdot V^2 = \text{const} \quad (1)$$

If you place a body in a uniform flow, the flow condenses just before the obstacle and is at the so-called pressure point (S2) in absolute rest. The total pressure of the flow can be measured at this point:

$$P_{\Sigma} = P_{Stat} + P_{Dyn} \quad (2)$$

The Itabar probe measures the average value of the total pressure using four holes on a streamlined surface. The holes on the back of the probe are subject to static pressure only. The difference between these two values serves as a measure of the flow velocity of the body.

$$\Delta P = P_{\Sigma} - P_{Stat} \quad (3)$$

Using the law of constancy, the flow rate can be calculated from the velocity and cross-sectional area:

$$\Delta P = P + \frac{\sigma}{2} \cdot V^2 - P_{Stat}, \quad V = \sqrt{\frac{2 \cdot \Delta P}{\sigma}} \quad (4)$$

Using the law of constancy, we can calculate the flow rate through the speed and cross-sectional area:

$$G = A \cdot \sqrt{\frac{2 \cdot \Delta P}{\sigma}} \quad (5)$$

In this way, the pressure drop is proportional to the square of the flow and is related to it through a certain probe shape-dependent coefficient DO, determined empirically. The precise calculation of the differential pressure created by the Itabar probe required for calibration is carried out at the factory using modern computing tools. The discrepancy with the manually calculated value is not so great, so the differential pressure value is quite accurate and can be used for the subsequent selection of a differential pressure transmitter, etc.

2. Microprocessor-based heat calculation

2.1. Calculation based on available heat sources

Basic dimensions and connection layout. The device is designed for mounting on the dashboard or panel board and can be built into separate cutouts in the panel or into open strips. Taking into account the available heat sources, make sure that the temperature between 0 and 50°C is maintained [7] Figure 3.

- Housing, connection
- Protection class (IP20 DIN 40050)
- Installation (control panel, panel)
- Connection (screw clamps)
- Dimensions (HxWxD) (144x72x220 mm)
- Weight (approx. 1.5 kg)

Limit values of errors:

1. basic heat error
 - - 20K<ΔT<100K 1%;
 - - 3K<Δ T<100° 1.5%
2. limit value of the temperature measurement error:
 - - ΔT > 20 K ± 0.1 K;
 - - 3K<Δ<20 K ±0.3 K;
 - limit values of the flow measurement error ± 0.5%.

Table 1
Technical characteristics of the devices

Entrances	
Temperature measurement	IMS in accordance with DIN IEC 751, in two- or four-wire versions from 0 to 200°
Temperature sensor	
Temperature range	
Measurement range for ΔT	$3K < \Delta T < 100^\circ C$
Flow measurement	
Input signal	0...20 mA or 4...20 mA
Input impedance	250 Ohms
Output	
Thermal energy, current	0...20 mA or 4...20 mA
Area	
Maximum resistance	500 Ohms
Pulse duration	≥ 50 ms

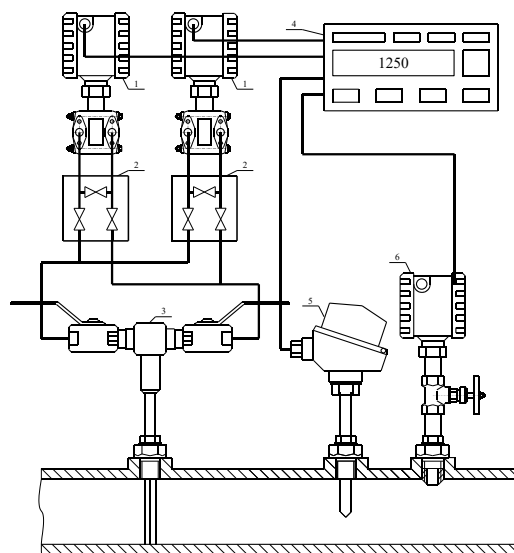


Figure 3: Multi-channel steam flow recording system (1 - flow sensor, 2 - valve block, 3 - ITARBAR-Sondo IBR-20, 4 - 2AR1600, 5 - temperature sensor, 6 - absolute pressure sensor).

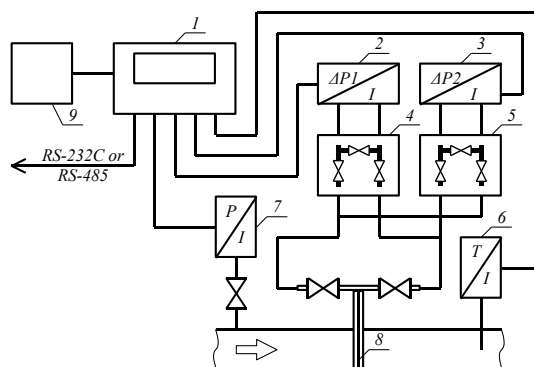


Figure 4: Process flow diagram of steam metering before the turbine (1 - computer-corrector (used for processing and storing information, as well as for generating and issuing control and reporting information); 2 - 3 - differential pressure sensor Sapphire 22-DD; 4 - 5 - three-way valve blocks; 6 - temperature sensor TTR or Pt-100; 7 - absolute pressure sensor Sapphire 22-AD; 8 - ITABAR probe; 9 - uninterruptible power supply unit).

Depending on the required flow measurement limit, from 1 to 3 differential pressure sensors and, accordingly, three-way valve blocks are used Figure 4.

IMS is understood as systems designed to automatically obtain quantitative information directly from the object under study by measuring and controlling, processing this information and issuing it in the form of a set of named numbers and statements, graphs, etc. reflecting the state of the object Figure 5.

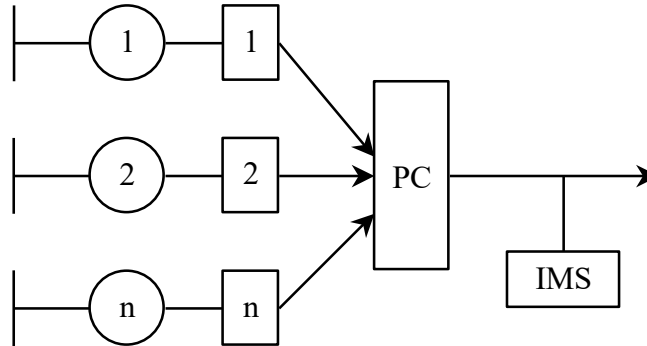


Figure 5: A typical structural diagram (PC - Primary Converter IMS - Information and Measuring Systems).

2.2. Development of an information control model for reactor power control

To create an IMS, it is necessary to clearly understand what information will be served by this system. It is important to know how much information about the monitored system X is provided by the observation of system Y [8] Figure 6.

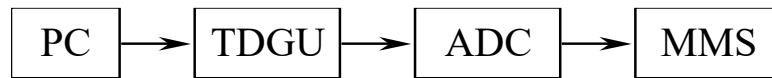


Figure 6: Block diagram of a single channel. (PC - Primary Converter TDGU - Temperature Difference Generation Unit ADC - Analog to Digital Converter MMS - Management of Measuring Systems).

The ITABAR type sensor is designed to measure the flow of liquid and gaseous media in pipelines from 15 mm to 12,000 mm.

- Output signal range 4÷ 20 mA.
- Input impedance of the channel converter, $R_{inc} \leq 250 \text{ Ohm}$.
- The controlled parameter is the steam flow to the turbine.

2.3. Calculation of parameters of a multichannel information and measurement system of a nuclear power plant

2.3.1. Calculation of the ADC bit depth

To calculate the ADC bit depth and subsequent calculations, you need to introduce a concept [9]:

The range of expected values of D

$$D = \frac{X_{max}}{X_{min}} = \frac{100\%}{20\%} = 5 \quad (6)$$

where X_{max} and X_{min} are the maximum and minimum power values corresponding to the maximum and minimum current of the detector.

Basic reduced channel error γ

$$\gamma_{dev} = \gamma_{add} + \gamma_{mult} \quad (7)$$

when measuring any quantity, it is impossible to obtain a signal free of distortion. The causes of these distortions can be different.

In measuring technology, the reduced error is used to estimate the reduced error, which consists of the additive error - independent of the value of the converted quantity, and the multiplicative error - proportional to the current value of the converted quantity. The reduced error of the measuring channel is defined by the following expression:

$$\gamma_{dev} = \gamma_{sens} + \gamma_{vb} + \gamma_{dd} + \gamma_{le} + \gamma_{ADC} \quad (8)$$

Where: γ_{sens} - sensor error, $\gamma_{sens} = 1\%$, γ_{vb} - error of the valve block, $\gamma_{vb} = 1\%$, γ_{dd} - error of the flow sensor Sapphire 22-DD, $\gamma_{dd} = 1\% - 0.25\%$, γ_{le} - communication line error, we accept $\gamma_{le} = 0.1\%$, γ_{ADC} - error of the analog-to-digital converter, $\gamma_{ADC} = 1\%$.

Then:

$$1\% + 1\% + 1\% + 0.1\% + 1\% = 4.1\% \quad (9)$$

As a result $\gamma_{add} = 2.05$, $\gamma_{mul} = 2.05$.

The ADC is designed to convert an analog signal into a digital signal. The ADC bit depth is determined taking into account the principle of uniform quantization of the dynamic range [10]:

$$q = \frac{x_2 - x_1}{2^n} \quad (10)$$

where q is the quantization value of the signal, $x_2 = I_{max}$ - maximum current value, $x_1 = I_{min}$ - minimum current value.

Quantization error:

$$\Delta_{quan} = \frac{1}{2} q \quad (11)$$

but on the other hand

$$\begin{aligned} \Delta_{quan} &= \gamma_{dev} \cdot I_{max} = 0.041 \cdot 2 \cdot 10^{-2} = 8.2 \cdot 10^{-4} \\ \frac{1}{2} q &= 8.2 \cdot 10^{-4} \\ q &= 4.1 \cdot 10^{-4} \\ \frac{I_{max} - I_{min}}{2^n} &= q \end{aligned} \quad (12)$$

Let's prologarithmize on the basis of 2:

$$n = \log_2 \frac{I_{max} - I_{min}}{q} = \log_2 \frac{2 \cdot 10^{-2} - 4 \cdot 10^{-3}}{4.1 \cdot 10^{-4}} \approx 5.3 < 6 \quad (13)$$

Thus, to ensure that the channel accuracy is not lower than the accuracy class of the sensor, it is necessary to use an ADC with a bit depth of six.

2.3.2. Calculation of the characteristics of reliability, reliability and efficiency of multichannel AIS functioning

To calculate the reliability characteristics, it is necessary to determine the equivalent number of graduations of a measuring device operating in the range of 4÷ 20 ma [11].

$$N_{eq}^{real} = \frac{\ln D_{exp}}{2 \gamma_{dev} \sqrt{D_{exp}}} = \frac{\ln 5}{2 \cdot 0.041 \cdot \sqrt{5}} = 8.9$$

$$N_{eq}^{id} = \frac{\ln D_{exp}}{2 \gamma_{dev}} = \frac{\ln 5}{2 \cdot 0.041} = 19.6$$
(14)

The probability of registering a signal from $D_{exp. 5}$ using a channel from $D_{exp. e^2}$:

$$P_{D_0} = \frac{N_{eq}^{real}}{N_{eq}^{id}} = \frac{8.9}{19.6} = 0.454$$
(15)

Probability of registering a signal with $D_{exp. 5}$ by a system of n measuring channels.

$$P_{D_c} = 1 - (1 - P_{D_0})^n$$
(16)

Table 2
Probability of signal registration

n	1	2	3	4	5	6	7	8
P_{D_c}	0,454	0,702	0,837	0,911	0,951	0,974	0,986	0,992

To calculate reliability characteristics, it is necessary to determine the failure rate. Failure rate of information channel elements λ_{DD} (technical documentation) [12]: $T_{DD} = 15000$ hours, $T_{ADC} = 10000$ hours.

$$\lambda_{Aver} = \lambda_{DD} + \lambda_{ADC} = \frac{1}{T_{DD}} + \frac{1}{T_{ADC}},$$

$$T_{Aver} = \frac{1}{\lambda_{DD} + \lambda_{ADC}} = \frac{1}{6.7 \cdot 10^{-5} + 3.3 \cdot 10^{-5}} = 10000 \text{ hours.}$$
(17)

CPI Failure Rate:

$$\lambda_{Aver} = \frac{1}{T_{Aver}} = 10^{-4}$$
(18)

Reliability for one subband:

$$P_{N_0} = \exp(-\lambda_{Aver} \cdot t_{an}) = \exp\left(-\frac{t_{an}}{T_{Aver}}\right) = 0.999$$
(19)

where $t_{an} = 7$ is the operating time on an autonomous power source.

The reliability of the system for the n th number of PKI is determined by the formula [13]:

$$P_N = (P_{N_0})^n$$
(20)

Table 3
System reliability

N	1	2	3	4	5	6	7	8
P_N	0,999	0,998	0,997	0,996	0,995	0,994	0,993	0,992

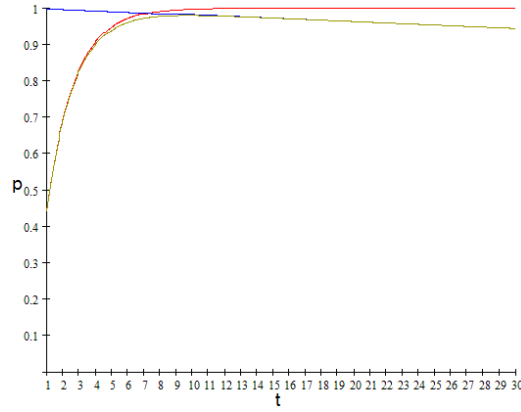


Figure 7: Validity (red curve), reliability (blue curve) and efficiency (purple curve).

Efficiency for the n-th number of sensors Figure 7:

$$W_{eff} = P_{N_0}^n \cdot [1 - (1 - P_{D_0})^n] \quad (21)$$

Let's enter the data into the table 4:

Table 4
Efficiency for n number of sensors

N	1	2	3	4	5	6	7	8
W_{eff}	0,426	0,700	0,835	0,907	0,947	0,968	0,979	0,988

By analyzing the obtained dependencies in a graph-analytical way, we will determine the optimal number of CPI, $n_{opt} = 8$.

2.3.3. Calculation of the energy characteristics of a multichannel IMS

This Figure 8 presents the scheme of a multi-channel Information and Measurement System (IMS). The diagram illustrates the flow and interaction between different components of the system.

- PC : Primary Converter, which initiates the process by converting the primary input.
- L : Leadership, managing the direction and control of the data flow.
- MT : Measuring Transducer, responsible for translating and processing measurements.
- MMS : Management of Measuring Systems, overseeing the system and ensuring accuracy and reliability.

This scheme highlights the importance of each component's role in optimizing the energy characteristics of the IMS, contributing to enhanced system reliability through functional duplication.

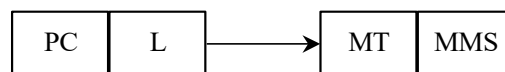


Figure 8: Scheme of a multi-channel IMS (PC - Primary Converter L - Leadership MT - Measuring Transducer MMS - Management of Measuring Systems).

The primary converter in our scheme is Sapphire 22-DD. Sapphire contains an amplifier. An approximate calculation of the signal coming from the strain gauge of the sapphire to the amplifier showed that the signal value is $0.3 \mu\text{A}$. From the primary converter, the signal is fed to the secondary converter. The secondary transducer and the MMS are technologically made in the same case and are microprocessor-based heat meters of the 2AP1600 type. In the primary converter, the signal is amplified ($3 \cdot 10^{-7}$) to the level perceived by the MMS ($4 \div 20 \text{ mA}$). The input resistance is equal to $R_{\text{inb.}} = 250 \text{ Ohms}$ [14].

Let's use Ohm's law to determine the voltage:

$$U = R \cdot I = 250 \cdot 3 \cdot 10^{-7} = 7.5 \cdot 10^{-5} \text{ V} \quad (22)$$

Signal Power Value is:

$$P = U \cdot I = 7.5 \cdot 10^{-5} \times 2 \cdot 10^{-2} = 1.5 \cdot 10^{-6} \text{ W} \quad (23)$$

The signal energy E_s will be determined from the formula:

$$E_s = (\gamma_{DD})^2 \cdot P \cdot t_u = 10^{-4} \cdot 1.5 \cdot 10^{-6} \cdot 5 \cdot 10^{-2} = 7.5 \cdot 10^{-12} \text{ J}, \quad (24)$$

where $\gamma_{DD} = 1\% = 10^{-2}$, $t_u \geq 5 \cdot 10^{-2}$ – cycle time for a given system.

2.3.4. Construction of the accuracy characteristic of a multichannel IMS

Accuracy - the number of divisions of the instrument scale that can be obtained. With the advent of digital computing, it is possible to quickly switch from one measurement limit to another. It is important to estimate the relative error of the instrument range [15].

$$\gamma = \frac{\Delta x}{x} \quad (25)$$

Since the error (accuracy class) of the sensor is equal to $\gamma = 1 \%$, the relative error

$$\gamma = \frac{\Delta x}{x} = 0.01 \quad (26)$$

Distribution price (quantization)

$$\Delta x = x_2 \cdot \gamma = 0.01 \quad (27)$$

Given that $\gamma = \gamma_{\text{add}} + \gamma_{\text{mul}} = 0.041$, we can see that [16]:

$$A = \frac{1}{2 \cdot \gamma_{\text{dev}}} = \frac{1}{2(\gamma_{\text{add}} + \gamma_{\text{mul}})} = \frac{1}{2\left(0.0205 + \frac{\Delta x}{x}\right)} \quad (28)$$

The obtained data are presented in Table 5.

Table 5
Function $A=f(x)$

x	0,1	0,2	0,3	0,4	0,5	0,6	0,7	0,8	0,9	1
A	4,149	7,092	9,288	10,99	12,35	13,45	14,37	15,15	15.82	16,40

The Figure 9 illustrates the accuracy characteristic of the system. The graph depicts the relationship between the variable x and the accuracy function $A(x)$, shown in red. The curve demonstrates how accuracy improves with changes in x , which is critical for assessing the efficiency

of function duplication in enhancing device reliability. Each vertical line represents key evaluation points important for understanding system performance within the specified range.

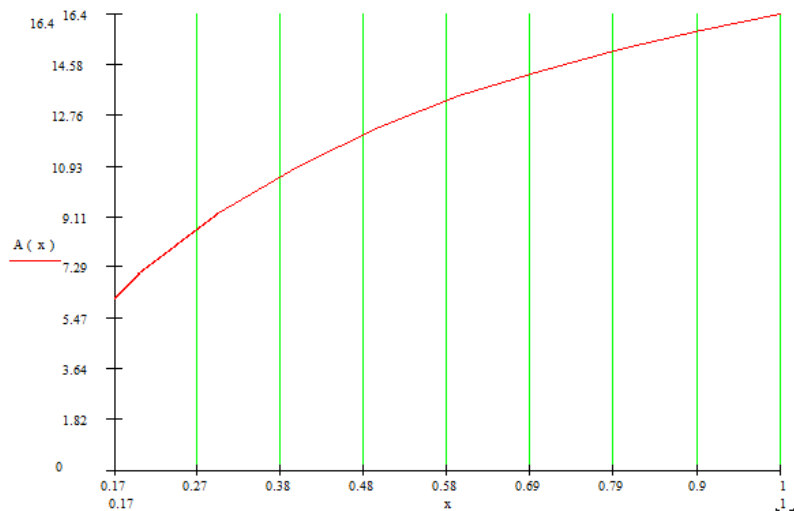


Figure 9: Accuracy characteristic.

3. Increase the reliability of the device when duplicating the functions of individual nodes

Monitoring the operation of both individual components and the device as a whole determines the efficiency of its operation and maintenance. Therefore, it is important to rely on an effective diagnostic system. Reliable operation of the operating parameter monitoring tool is influenced not only by the reliability of individual components, but also by the way they are combined in the measuring device. Since the distribution laws for the equipment life cycle and recovery time in the event of a failure are subject to an exponential distribution, the method of differential equations can be used to estimate the reliability of the process of determining a critical operating parameter based on the graph of states of the system under study in which it can be in during failures and recoveries, and statistical data on the average uptime or recovery time [17, 18].

In particularly important cases, to prevent abnormal situations, duplication of individual monitoring functions by several sensors is used. Let's consider how this technique affects the reliability of the measuring unit as a whole. We assume that: - failed objects are immediately restored, there are no restrictions on the number of restorations.

To build the corresponding system of differential equations, consider the state graph of the redundant measuring system, which reflects the possible directions of transitions from one state to another. The logical scheme of interaction of the duplicated system of refrigerant flow sensors is shown in Figure 10.

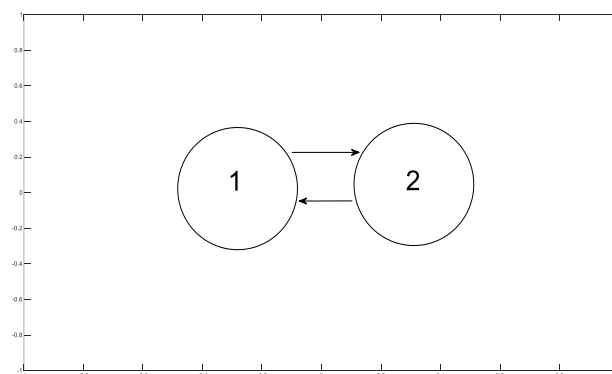


Figure 10: State graph of duplicate sensors.

The system can be in two states: "Agent 1 flow sensor is activated" or "Agent 2 flow sensor is activated". Each of the transitions corresponds to a transition intensity value: $l = 1/T$ to failure and $m = 1/T$ to recovery. Based on the state graph, we form the equation:

- on the left side of each equation is the time derivative of the probability of the system being in the j th state at time t ;
- the number of terms on the right-hand side is equal to the number of connections that affect this state;
- each such term is equal to the product of the transition intensity and the probability of the initial state (the one from which the arrow leaves in the state graph). The sign of the product is positive if the arrow enters the state under consideration and negative if it leaves it;
- the number of equations is equal to the number of system states.

The system of differentiations for the values of the intensity coefficients inverse to the operating time and downtime $l_i = \frac{1}{T_i}$ before failure and $m = \frac{1}{T_i}$ before recovery is constructed according to the given logical scheme:

$$\frac{dp_1(t)}{dt} = -m_1 p_1(t) - l_2 p_2(t) \quad (29)$$

$$\frac{dp_2(t)}{dt} = l_1 p_1(t) - m_2 p_2(t) \quad (30)$$

which is supplemented by a condition:

$$p_1(t) + p_2(t) = 1 \quad (31)$$

The probability that both or one of the two sensors will be in good working order

$$P(t) = p_1(t)(1 - p_2(t)) + p_2(t)(1 - p_1(t)) \quad (32)$$

To find a solution to system (29-30) and calculate (32), we constructed the corresponding S-model in MATLAB SMULNK, which is shown in Figure 11.

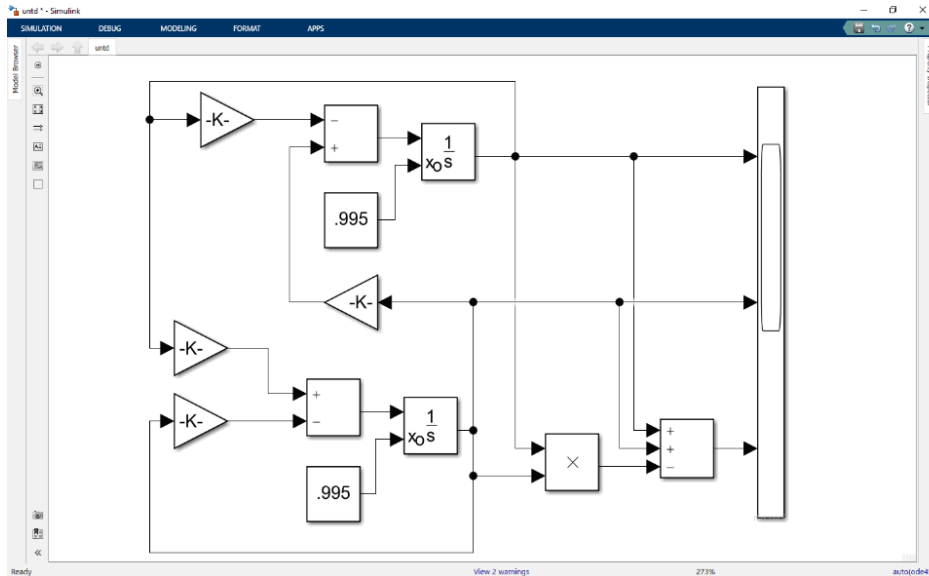


Figure 11: S-model for finding a solution to the probabilistic model and assessing the reliability of a node with duplicate blocks.

The change of $p_1(t)$, $p_2(t)$ and $P(t)$ with the time of operation of the detector is shown in Figure 12 in yellow, blue and red colors, respectively.

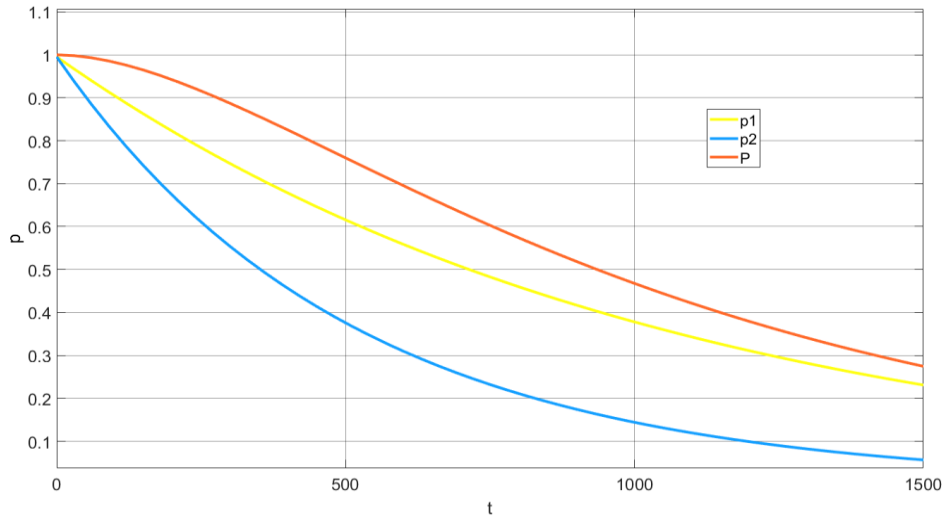


Figure 12: Changes in the probabilities of $p_1(t)$, $p_2(t)$ for each of the sensors in standalone mode and $P(t)$ when they are used in parallel.

The change in the detector operating time is shown in Figure 12. It uses yellow, blue, and red colors. Each color represents a change in probability over time.

Conclusions

The calculation of a multichannel adaptive information and measuring system for measuring steam flow into a turbine using the ITABAR probe is investigated.

1. Increase reliability through duplication: Duplication of key functions of individual nodes provides increased fault tolerance. This allows the system to continue to function even if one component fails, which is important for mission-critical applications such as steam flow measurement in turbines.
2. Optimization of component interaction: By optimally designing the interaction between duplicate components, it is possible to achieve not only increased reliability, but also a reduction in the overall workload of each individual component. This can also have a positive impact on the life of the system as a whole.
3. Using the S-model: A modeling tool such as the S-model allows for a more accurate assessment of system reliability by simulating a variety of failure and recovery scenarios. This creates an opportunity to improve the system during the design phase, reducing the risk of real-world failures.
4. Adaptive capabilities: An adaptive system architecture can automatically reroute data flows in the event of a component failure. This makes the system more flexible and able to maintain high measurement accuracy under any conditions.
5. Economic aspects: While the initial cost of duplicating components may be higher, the long-term savings from reduced downtime and maintenance can be a significant benefit. Investments in reliability can provide significant cost savings in the future.
6. Improving the overall quality of the system: Implementing duplication of functions as a standard approach can improve the overall quality and efficiency of the system so that it can meet higher standards of reliability and safety.

Declaration on Generative AI

The authors have **not employed any Generative AI tools**.

References

- [1] N.G. Leveson Engineering a Safer World: Systems Thinking Applied to Safety, MIT Press, 2016.
- [2] Popov, Emil, and Todor Andreev, Reliability Engineering and its Application in Critical Digital Industrial Applications, Springer, 2019.
- [3] B.M. Ayyub, and R. H. McCuen, Probability, Statistics, and Reliability for Engineers and Scientists, CRC Press, 2016.
- [4] A. Mosleh, and R. C. Kuo, Reliability and Risk Issues in Large Scale Safety-critical Digital Control Systems, Springer, 2020.
- [5] H.J. Krauss and H. Prokop Measurement and Control Basics, CRC Press, 2021.
- [6] M. Bertolini, et al, Engineering Methods in the Service-Oriented Design of Systems on Reliability Management, Springer, 2018.
- [7] B. Schwarz, and K. Lars, Adaptive Measurement Systems: Applications and Techniques in Adaptive Control, John Wiley & Sons, 2019.
- [8] W.S. Hung, and A. Z. Nor, Measurement Uncertainty Analysis, Springer, 2018.
- [9] Z.-Y. Sun, et al., Reliability Analysis and Testing Requirements in Industry, Industrial & Science Press, 2016.
- [10] K. P. Vikash, Digital Signal Processing Handbook, CRC Press, 2019.
- [11] A. Milani, Thermo-engineering and the application of measurement systems in complex environments, Springer, 2020.
- [12] K. Dubey, and K. Santosh, Advances in Instrumentation & Measurement: Industrial Innovations for Controlling Complex Systems, CRC Press, 2021.
- [13] C. Tan, X. Pan, Control and Measurement Engineering for Energy Systems, CRC Press, 2020.
- [14] W. Guoxin, L. Zhifeng, Multiple Channel Control Systems: Design, Implementation and Measurement Techniques, Springer, 2019.
- [15] T. Hovorushchenko, D. Medzaty, Yu. Voichur, M. Lebiga Method for forecasting the level of software quality based on quality attributes. Journal of Intelligent & Fuzzy Systems. (2023). 44 3 3891-3905.
- [16] T. Hovorushchenko, O. Pavlova, V. Avsiyevych. Method of Assessing the Impact of External Factors on Geopositioning System Operation Using Android GPS API, Proceedings of 2021 IEEE International Scientific and Technical Conference, Computer Science and Information Technologies, CSIT-2021, Lviv-Zbarazh, Ukraine, September 22-25, 2021, pp. 295-298.
- [17] V. Martsenyuk, A. Sverstiuk, T. Dubynyak, P. Mykulyk, N. Shostakivska and M. Poshyvak. Study of the temperature effect on the functioning of photodetecting lighting elements and calculation of their reliability, 1st International Workshop on Intelligent and CyberPhysical Systems, ICyberPhyS 2024, Khmelnytskyi Volume 3736, Pages 30 - 46, 2024
- [18] A. D. Wood, and J.D. Richard Phillips, Multichannel Measurement Systems: Theory and Applications, Taylor & Francis, 2018.